

INTERFACE CONDITIONS MODELLING IN COMPUTATIONAL LIMIT ANALYSIS

A.V. Lyamin

Centre for Geotechnical and Materials Modelling, University of Newcastle, Australia

K. Krabbenhøft

Centre for Geotechnical and Materials Modelling, University of Newcastle, Australia

S.W. Sloan

Centre for Geotechnical and Materials Modelling, University of Newcastle, Australia

ABSTRACT: *In many geotechnical stability problems it is important to account for interface conditions between soil and structure, e.g. retaining walls and footings with no-tension contact. These interfaces can be considered as discontinuities in stress and velocity fields developed in the system undergoing plastic collapse. Discontinuous variable fields are often employed in FE lower and upper bound limit analyses to improve the performance of lower order elements used to obtain rigorous bounds on the collapse factor. Recently it was shown that these discontinuities can be conveniently represented by a patch of regular elements of zero thickness. This development opens the way for discontinuous LA formulations to be used with general yield criteria in both two- and three-dimensions to solve stability problems involving a wide variety of materials and interface conditions.*

1 DISCRETE FORMULATION OF BOUND THEOREMS

Consider a domain Ω with boundary Γ , as shown in Fig. 1. Let \mathbf{t} and \mathbf{q} denote, respectively, a set of fixed tractions acting on the part of the boundary Γ_f , and a set of unknown tractions acting on the part of the boundary Γ_q . Similarly, let \mathbf{g} and \mathbf{h} be a system of fixed and unknown body forces which act, respectively, on the volume Ω . Under these conditions, the objective of a lower bound calculation is to find a stress distribution which satisfies equilibrium throughout Ω , balances the prescribed tractions \mathbf{t} on Γ_f , nowhere violates the yield criterion, and maximises the integral

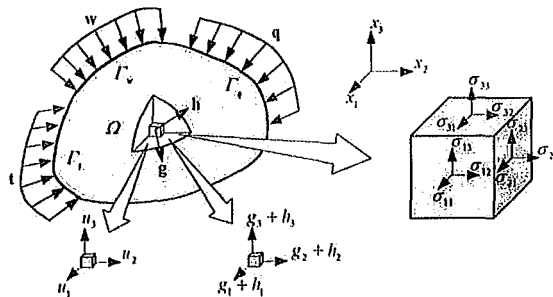


Fig. 1. A domain subject to a system of surface and body forces.

$$Q = \int_{\Gamma_q} \mathbf{q} d\Gamma + \int_{\Omega} \mathbf{h} d\Omega \quad (1)$$

The objective of an upper bound calculation is to find a velocity distribution \mathbf{u} which satisfies compatibility, the flow rule, the velocity boundary conditions \mathbf{w} on the surface area Γ_w , and minimises the integral

$$W^{internal} = \int_{\Omega} \boldsymbol{\sigma} \dot{\boldsymbol{\epsilon}} d\Omega \quad (2)$$

An upper bound estimate on the true collapse load can be obtained by equating $W^{internal}$ to the power dissipated by the external loads

$$W^{external} = \int_{\Gamma_t} \mathbf{t}^T \mathbf{u} d\Gamma + \int_{\Gamma_q} \mathbf{q}^T \mathbf{u} d\Gamma + \int_{\Omega} \mathbf{g}^T \mathbf{u} d\Omega + \int_{\Omega} \mathbf{h}^T \mathbf{u} d\Omega \quad (3)$$

To preserve the bounding properties of the numerical solutions, linear finite elements are used to discretise the continuum. In an effort to provide the best possible bounds, kinematically admissible velocity discontinuities and statically admissible stress discontinuities are permitted at all inter-element boundaries for, respectively, the upper and lower bound analyses (Sloan and Kleeman, 1995; Sloan, 1988). These discontinuities allow accurate estimates of the collapse load to be computed without using an excessive number of elements and can be efficiently implemented using the approach described in following sections.

2 VELOCITY DISCONTINUITIES AS A PATCH OF THIN ELEMENTS

A general approach for modelling a discontinuous velocity field in D dimensions, regardless of the yield criterion involved, can be derived by treating a discontinuity as a patch of D infinitely-thin elements (Krabbenhøft et al., 2005). The problem model is then simplified because the power dissipation given by (2) can be computed as the sum of contributions from all elements in the mesh. We will next show that using linear finite elements for the problem discretisation results in an a priori simplification for velocity discontinuities which are valid for general yield criteria.

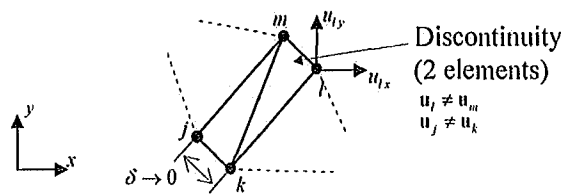


Fig. 2. Discontinuity as a patch of interconnected thin elements – upper bound.

For illustrative purposes let us consider a two-dimensional patch of interconnecting triangles shown in Fig. 2. Each triangle is a constant stress-linear velocity element with the velocity vector, \mathbf{u} , varying according to

$$\mathbf{u} = \sum_i N_i(x, y) \mathbf{u}_i, \quad N_i(x, y) = \frac{a_i + b_i x + c_i y}{2\Delta} \quad (4)$$

where Δ is the area of the triangle and coefficients a , b , c are computed from nodal

coordinates as follows

$$a_k = x_l y_m - x_m y_l, \quad b_k = y_l - y_m, \quad c_k = x_m - x_l \quad (5)$$

for node k and then with cyclic interchanges of indexes for nodes l and m . The compatibility matrix \mathbf{B} is given by

$$\mathbf{B} = [\mathbf{B}_k \ \mathbf{B}_l \ \mathbf{B}_m] = \frac{1}{2\Delta} \begin{bmatrix} b_k & 0 & b_l & 0 & b_m & 0 \\ 0 & c_k & 0 & c_l & 0 & c_m \\ c_k & b_k & c_l & b_l & c_m & b_m \end{bmatrix} = \frac{1}{\Delta} [\bar{\mathbf{B}}_k \ \bar{\mathbf{B}}_l \ \bar{\mathbf{B}}_m] = \frac{1}{\Delta} \bar{\mathbf{B}} \quad \text{or} \quad \bar{\mathbf{B}} = \mathbf{B}\Delta \quad (6)$$

and the power dissipated in any triangular element, regardless of its area, is calculated from

$$W = \int_{\Delta} \boldsymbol{\sigma} \dot{\boldsymbol{\varepsilon}} d\Delta = \int_{\Delta} \boldsymbol{\sigma} \mathbf{B} \mathbf{u} d\Delta = \boldsymbol{\sigma} \bar{\mathbf{B}} \mathbf{u} = \boldsymbol{\sigma} \dot{\boldsymbol{\varepsilon}} \quad (7)$$

The flow rule can be presented in a similar way as

$$\bar{\mathbf{B}} \mathbf{u} = \Delta \times \dot{\lambda} \nabla f(\boldsymbol{\sigma}) = \dot{\lambda} \bar{\nabla} f(\boldsymbol{\sigma}) \quad (8)$$

Considering now the case of an infinitely thin element with side lm being collapsed, we find that $\bar{\mathbf{B}}_k \rightarrow \mathbf{0}$ and $\bar{\mathbf{B}}_l \rightarrow -\bar{\mathbf{B}}_m$, resulting in the compatibility matrix

$$\hat{\mathbf{B}} = [\mathbf{0} \ -\bar{\mathbf{B}}_{lm} \ \bar{\mathbf{B}}_{lm}] \quad (9)$$

where $\bar{\mathbf{B}}_l$ has been replaced by $\bar{\mathbf{B}}_{lm}$ for notation convenience. It is readily seen that the strain rate in element k, l, m in this case can be expressed in terms of differences between velocities (velocity jumps) at nodes l and m leading to

$$\dot{\boldsymbol{\varepsilon}} = \hat{\mathbf{B}} \mathbf{u} = \bar{\mathbf{B}}_{lm} \Delta \mathbf{u}^{lm} \quad (10)$$

Krabbenhøft et al. (2005) showed that expression (10), when employed for a Mohr-Coulomb criterion, leads to the conventional expressions for the flow rule and power dissipation in the discontinuities. But modelling the discontinuities as patches of infinitely thin elements avoids any need for special treatment. Indeed, the power dissipation is computed using (7) and the flow rule constraints are given by (8). These constraints are actually obtained automatically as part of the system of optimality conditions for the upper bound optimization problem.

3 STRESS DISCONTINUITIES AS A PATCH OF THIN ELEMENTS

An efficient lower bound formulation requires statically admissible stress discontinuities between adjacent elements (Fig. 3). The constraints for these discontinuities are that only

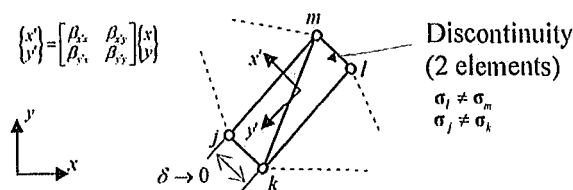


Fig. 3. Discontinuity as a patch of interconnected thin elements – lower bound.

normal and shear stresses must be continuous across the inter-element boundary. We now show that this requirement is equivalent to the element equilibrium conditions written for the discontinuity elements in the patch. Using the notation introduced in the previous section, the equilibrium conditions for element k, l, m can be written as

$$\mathbf{B}^T \boldsymbol{\sigma} = \begin{bmatrix} \mathbf{B}_k^T & \mathbf{B}_l^T & \mathbf{B}_m^T \end{bmatrix} \begin{Bmatrix} \boldsymbol{\sigma}^k \\ \boldsymbol{\sigma}^l \\ \boldsymbol{\sigma}^m \end{Bmatrix} = \frac{1}{\Delta} \begin{bmatrix} \bar{\mathbf{B}}_k^T & \bar{\mathbf{B}}_l^T & \bar{\mathbf{B}}_m^T \end{bmatrix} \begin{Bmatrix} \boldsymbol{\sigma}^k \\ \boldsymbol{\sigma}^l \\ \boldsymbol{\sigma}^m \end{Bmatrix} = -(\mathbf{g} + \mathbf{h}) \quad (11)$$

which is equivalent to

$$\begin{bmatrix} \bar{\mathbf{B}}_k^T & \bar{\mathbf{B}}_l^T & \bar{\mathbf{B}}_m^T \end{bmatrix} \begin{Bmatrix} \boldsymbol{\sigma}^k \\ \boldsymbol{\sigma}^l \\ \boldsymbol{\sigma}^m \end{Bmatrix} = -(\mathbf{g} + \mathbf{h})\Delta \quad (12)$$

For a zero volume element with side lm being collapsed, Eqn. (12) becomes

$$\begin{bmatrix} \mathbf{0} & -\bar{\mathbf{B}}_{lm}^T & \bar{\mathbf{B}}_{lm}^T \end{bmatrix} \begin{Bmatrix} \boldsymbol{\sigma}^k \\ \boldsymbol{\sigma}^l \\ \boldsymbol{\sigma}^m \end{Bmatrix} = \mathbf{0} \quad \text{or} \quad \bar{\mathbf{B}}_{lm}^T \boldsymbol{\sigma}^l = \bar{\mathbf{B}}_{lm}^T \boldsymbol{\sigma}^m \quad (13)$$

The last of equations (13) represents the equality of surface tractions between nodes l and m . After dividing the coefficients b_l and c_l of matrix $\bar{\mathbf{B}}_{lm}$ by the length of the discontinuity L , we obtain the direction cosines $\beta_{x'x}, \beta_{x'y}$ for the axis x' . Thus (11) finally leads to

$$\begin{Bmatrix} t'_x \\ t'_y \end{Bmatrix} = \begin{Bmatrix} t'_x \\ t'_y \end{Bmatrix} \quad (14)$$

Application of the conditions (14) is equivalent to setting the normal/shear stresses to be equal at nodes l and m , as these are linearly related to surface tractions by

$$\begin{Bmatrix} \sigma'_n \\ \sigma'_t \end{Bmatrix} = \begin{bmatrix} \beta_{x'x} & \beta_{x'y} \\ \beta_{y'x} & \beta_{y'y} \end{bmatrix} \begin{Bmatrix} t'_x \\ t'_y \end{Bmatrix} \quad (15)$$

Therefore, the approach of treating discontinuities as a patch of zero volume elements also suits the lower bound formulation, as no special "discontinuity constraints" need to be introduced. Indeed, simple application of the familiar equilibrium conditions is sufficient to ensure that the discontinuity is statically admissible.

4 INTERFACES MODELLING

4.1 Interfaces Between Material Domains

The arrangement of the elements at an interface and the locations of the stress and velocity nodes are presented in Fig. 4. Assuming an associated flow rule, the interface conditions are governed by the yield function in the zero thickness elements. For upper bound analysis, only one layer of discontinuity elements in the interface is needed as these elements have

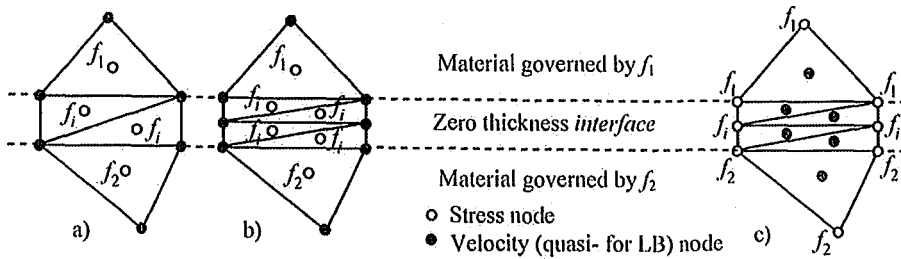


Fig. 4. Interface layout for upper (a), (b) and lower (c) bound formulations.

separate stress variables (Fig. 4a). For lower bound meshes this is not the case and two layers of zero thickness elements are essential to prescribe material properties to the stress points which are separate from the stress points of the domains adjoining the interface. To make the patch symmetric, two layers of elements are used by default for both lower and upper bound limit analysis in proposed implementation.

To demonstrate the feasibility of the approach the plane strain collapse of a surface footing on clay subjected to vertical eccentric loading (Fig. 5) is considered. Two kinds of interface conditions are modelled: full adhesion and tension cut off. The collapse mechanisms shown and corresponding bearing capacity values demonstrate the influence of the tension cut-off condition.

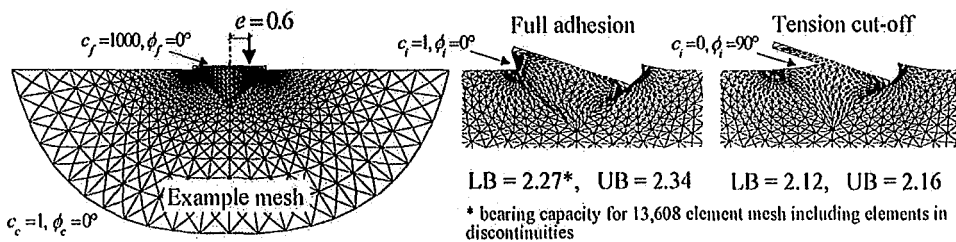


Fig. 5. Strip footing on clay subject to eccentric ($e=0.6$) loading with full adhesion and tension cut-off interface conditions.

4.2 Interfaces at Segments Subject to Boundary or Loading

Modelling of surface effects under applied loading or boundary conditions can proceed in the same manner as it was done for implementing the interfaces between materials. Furthermore, only one layer of zero thickness elements is sufficient in this case as we already have stress nodes which are “outside” of the domain. Therefore, for these nodes any desired yield conditions can be applied without interference with the material assumed for the domain itself (Fig. 6).

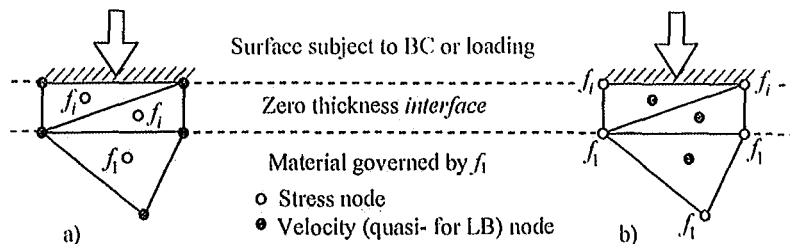


Fig. 6. Surface interface layout for upper (a) and lower (b) bound formulations.

The simple example of vertical loading of a cohesive-frictional ($c=1, \phi=20^\circ$) rectangular block laying on a flat surface is used (Fig. 7) to show a few possible scenarios of using the element patch interfaces between the applied loading or boundary and the problem domain. Three different cases of interface conditions are modeled with corresponding collapse mechanisms and limit loads shown in Fig. 7.

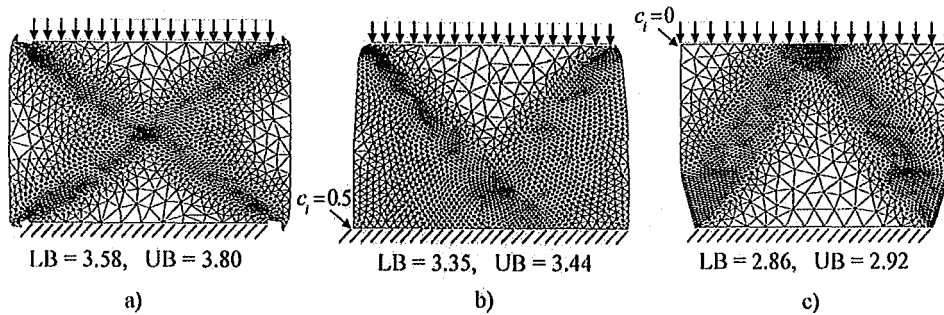


Fig. 7. Collapse of rectangular block ($H/B=0.8$) subject to rigid vertical loading with:
a) rough top/rough bottom; b) rough top/partially rough bottom; c) smooth top/rough bottom.

4.3 Interfaces for Overlapping Connections

Quite often in geotechnical engineering a series of plane strain stability analyses is performed on critical sections of the original 3D problem to make the case computationally feasible. This practice is common for such problems as the bearing capacity of foundations and the stability of dams, slopes and retaining walls. For anchor supported retaining walls, a problem arises in the modelling of anchors/ties without simultaneously introducing an artificial reinforcement effect. One efficient solution is to take the connection between the wall and the anchor “out” of the soil and make it overlap. This requires a special connection interface

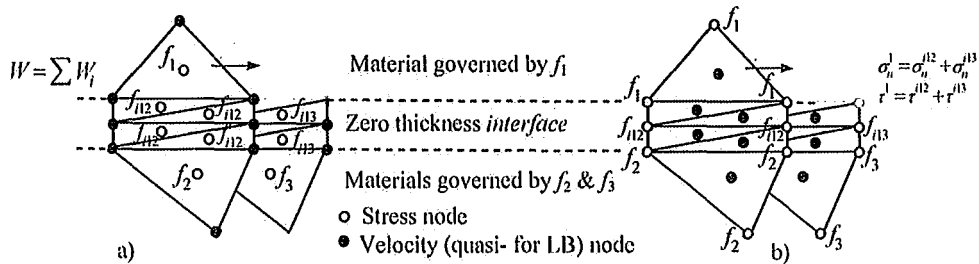


Fig. 8. Dual connection interface for upper (a) and lower (b) bound formulations.

which preserves the wall interaction with the soil and at the same time connects it to the anchor tie. Such complex connections can be modelled efficiently by using multilayered zero thickness patches of elements, as shown in Fig. 8. The upper bound implementation of multilayered interfaces is straightforward, as the power dissipated at the interface is just a sum of powers dissipated in all interface elements. For a lower bound analysis, a small adjustment is needed to the single layer implementation. In this case, the shear and normal tractions for nodes on the unsplit side must be equal to the sum of the shear and normal tractions of each of the layers (Fig. 8 b).

Fig. 9 shows an anchored sheet pile wall with the anchor tie implemented as a) interacting with the surrounding soil and b) overlapping the soil with a double-layered interface connection to the wall. The dual layer connection interface employed for this problem also includes a moment free wall/tie connection and no-tension conditions between the wall and the adjacent soil. The difference in the collapse pattern and bound values underlines the importance of selection the model appropriately.

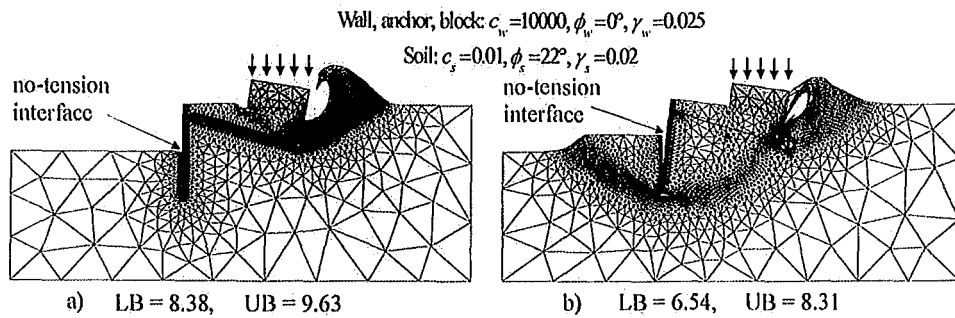


Fig. 9. Building with anchored sheet pile wall support: a) anchor tie is in contact with soil, b) anchor tie overlaps the soil and is connected to the wall using dual layer interface.

4.4 Moment-Free Interfaces for Joints Modelling

Usually structural elements have to be used to model joints with rotation. However, moment free connections can be implemented without any special elements by applying equality constraints on the stresses and velocities of the surface nodes of adjoining domains as shown in Fig. 10. These constraints ensure force and moment equilibrium across the joint for static formulations and rigid segment rotation for kinematic formulations, thus preserving the rigor of both lower and upper bound analyses.

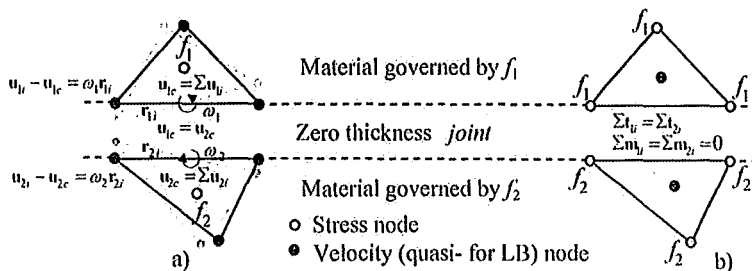


Fig. 10. Moment free joint constraints for upper (a) and lower (b) bound formulations.

The case of dual leg footing failure is used here to check the implementation of joints for limit analysis applications (Fig. 11). Two extreme cases are considered: a) the foundation panel is fully attached to the legs; b) the panel is attached to the legs via moment free joints. The load applied is inclined at 30 degrees to the horizontal, thus inducing quite distinctive

modes of collapse, namely sliding and rotational failure, as shown in Fig. 11 a) and b).

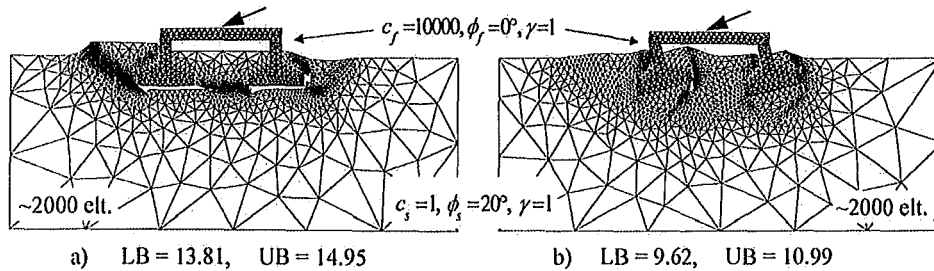


Fig. 11. Failure of panel resting on pair of footing legs and subject to inclined (30°) loading: panel is fully attached to footings, b) panel is attached via moment free joints.

CONCLUSIONS

A novel approach for modelling interface in the framework of numerical limit analysis has been presented. The method is based on a patch of zero thickness “solid” elements of regular topology with the properties of the interface material governed by the assumed yield criterion enforced at the corresponding stress points. Since all the conditions of the limit theorems are satisfied, the resultant kinematic and static formulations furnish rigorous upper and lower bounds and can be used for two- and three-dimensional stability problems with various interface conditions that are governed by general types of yield criteria.

REFERENCES

- Krabbenhøft K., Lyamin A.V., Hijaj M., Sloan S.W. (2005), “A new discontinuous upper bound limit analysis formulation”. *Int. J. Num. Meth. Eng.*, Vol. 63, 1069-1088.
- Lyamin A.V., Krabbenhøft K., Abbo, A.J., Sloan S.W. (2005), “General approach to modelling discontinuities in limit analysis”. *Proceedings of IACMAG 11, Turin*.
- Sloan S.W. and Kleeman P.W. (1995), “Upper bound limit analysis using discontinuous velocity fields”. *Comp. Meth. Appl. Mech. Eng.*, Vol. 127, 293-314.
- Sloan S.W. (1988), “Lower bound limit analysis using finite elements and linear programming”. *Int. J. Num. Anal. Meth. Geomech.*, Vol. 12, 61-77.